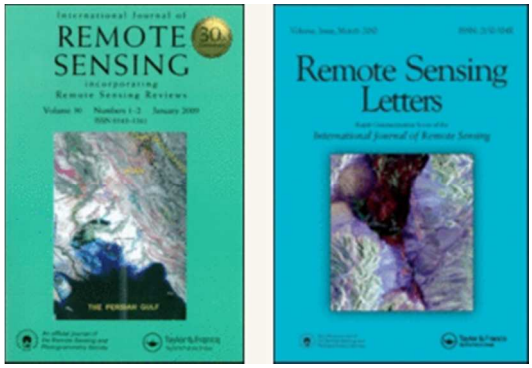

Detection of olive oil mill waste (OOMW) disposal areas in the island of Crete using freely distributed high resolution GeoEye's OrbView-3 and Google Earth images

Journal:	*International Journal of Remote Sensing*
Manuscript ID:	TRES-LET-2015-0196
Manuscript Type:	RSL Research Letter
Date Submitted by the Author:	20-May-2015
Complete List of Authors:	Agapiou, Athos; Cyprus University of Technology, Civil Engineer and Geomatics; Institute for Mediterranean Studies, Foundation for Research & Technology, Hellas (F.O.R.T.H.), Laboratory of Geophysical-Satellite Remote Sensing & Archaeo-environment Papadopoulos, Nikos Sarris, Apostolos; Foundation for Research & Technology (FORTH), Institute for Mediterranean Studies
Keywords:	classification, image analysis
Keywords (user defined):	olive mill waste water areas, disposal areas, GeoEye OrbView-3 / Google Earth

Detection of olive oil mill waste (OOMW) disposal areas in the island of Crete using freely distributed high resolution GeoEye's OrbView-3 and Google Earth images

Athos Agapiou[a,b], *Nikos Papadopoulos*[b], *Apostolos Sarris*[b]

[a] *Department of Civil Engineering and Geomatics, Faculty of Engineering and Technology, Cyprus University of Technology, 2-6, Saripolou str., 3603, Limassol, Cyprus, athos.agapiou@cut.ac.cy*

[b] *Laboratory of Geophysical-Satellite Remote Sensing & Archaeo-environment, Institute for Mediterranean Studies, Foundation for Research & Technology, Hellas (F.O.R.T.H.), asaris@ret.forthnet.gr*

ABSTRACT

This paper aims to examine the potential use of freely distributed satellite images for the detection of Olive oil mil waste (OOMW) areas in the island of Crete. Two cases studies have been selected in Crete. In the first case study area an archive GeoEye OrbView-3 image was used so as to detect OOMW areas using Spectral Angle Mapper detection algorithm and other geometric and topographic parameters. In the second case study, Google Earth images have been examined trough different classification algorithms in different scales. The overall results demonstrate that remote sensing techniques may be used as an alternative way to detect and therefore monitor OOMW areas while freely RGB distributed images from digital globes (such as Google Earth) can be sufficiently used for this purpose.

Keywords: olive mill waste water; disposal areas, GeoEye OrbView-3; Google Earth; classification

1. INTRODUCTION

There are approximately 750 million productive olive trees worldwide, 98% of them located in the Mediterranean region, where more than 97% of olive oil is produced. The three major olive oil producers worldwide are Spain, Italy, and Greece (Asfi et al., 2012; Roig, Cayuela and Sánchez-Monedero, 2006). Indeed, olive oil industry is very important in Mediterranean countries, both in terms of wealth and tradition. Olive oil industry is considered to be as one of the driving sectors of the agricultural economy of the Mediterranean basin. However, the extraction of olive oil generates huge quantities of wastes that may have a great impact on land and water environments due to high phytotoxicity. Several studies have proven the negative effects of these wastes on soil microbial populations (Paredes et al., 1987) or on aquatic ecosystems (DellaGreca et al., 2001). In addition to solid waste generated in the olive groves by annual pruning of olive trees, a significant amount of solid waste is generated during milling in the form of leaves and small twings brought to the mill with the olives and in the form of crushed olive stones and sizeable remnants of olive pulp following olive oil extraction. Leaves and twigs can be used as animal feed or in the production of compost after mixing with other appropriate materials (Niaounakis and Halvadakis, 2006). Liquid waste is known as olive-mill wastewater (OMWW), since during olive milling and olive oil extraction substantial amounts of added water as well as olive juice. From an environmental point of view OMWW is the most critical waste emitted by olive-mills in terms of quantity as

well quality. Indeed pollution from olive oil production is often a problem in poor communities where sophisticated solutions to the problem are too expensive (Niaounakis and Halvadakis, 2006). OMW uncontrolled disposal areas in aquatic and terrestrial receptors is associated with detrimental effects because of their high content in salts and in organic matter. As a consequence, OMW can inhibit plant and microbial growth, alter soil fungal and bacterial communities' structure as well as soil physicochemical properties (Ntougias et al., 2013). OMW are difficult to be documented due to their seasonal operation as well their high territorial scattering.
Remote sensing images may provide a systematic and cost-effective methodology in order to identify as well to monitor open air OMW disposal areas. The distribution of freely available satellite images can be used in order to support such actions and assist local authorities to control OMW disposal areas. Therefore this paper aims to investigate the contribution of freely high resolution satellite images from Google Earth platform as well archive GeoEye OrbView-3 images in order to detect OMW disposal areas. So far, a very limited number of studies have been conducted to map OMW from freely available images such as Google Earth. As the first endeavour in this direction, this paper explores the feasibility of using the freely available images from Google Earth and GeoEye OrbView-3 to classify and detect OMW disposal areas.

2. CASE STUDY AREA

The area of olive groves in Greece has increased constantly during the last quarter of the century, as a result of the planting of new high-density groves, reaching an area of about 8.336 km2 in 2007 (+120.000 ha since 1991). Olive groves have expanded in many semi-mountainous and coastal areas mainly in Crete and Peloponnese (Camarsa et al., 2010). Greece holds the third place worldwide in the olive oil production and the island of Crete contributes approximately 5% to the total world olive oil production (Alexakis et al., 2015). For the aims of this paper, two areas of interest have been selected (Figure 1). The first area (*case study area 1: Mesaras inlet*) is located in the southern-central part of Crete while the second case area (*case study 2: Mironikitas* area) is focused in the northern western part of Crete.

Figure 1: The two cases studies area in the island of Crete. The 1st case study (indicated with yellow square in the central-southern part of Crete) a high resolution GeoEye OrbView-3 satellite image was used while for the 2nd case study (indicated with yellow square in the eastern-northern part of Crete) GE images have been explored.

3. RESOURCES AND METHODOLOGY

a. Case study area 1: *Mesaras* inlet

For the 1st case study area located in the *Mesaras* inlet, a GeoEye's OrbView-3 image was used. GeoEye's OrbView-3 satellite was among the world's first commercial satellites to provide high-resolution imagery from space. OrbView-3 collected one meter panchromatic (black and white) or four meter multispectral (NIR-R-G-B) imagery at a swath width of 8 km for both sensors. The U.S. Geological Survey (USGS) Earth Resources Observation and Science (EROS) received 179,981 OrbView-3 image "segments" from GeoEye with no restrictions. The data were delivered in Basic Enhanced (Level 1B) radiometric corrected format. The product files include satellite telemetry data, rational functions, post-processed Ground Sample Distance (GPS) at nadir data, and sufficient metadata for rigorous triangulation. The data in this collection were acquired between September 2003 and March 2007, from the multispectral (MS)

and panchromatic (Pan) sensors. Over 84% of the Orbview-3 collection is PAN (USGS, 2012). The methodology followed in this area was focused to the semi-automatic identification of OMW disposal areas based on seven (7) steps:

Step 1: Orthorectification. The GeoEye OrbView-3 image was initially orthorectified using Rational Polynomial Coefficients (RPC) and ASTER Global Digital Elevation Model (ASTER GDEM) data. The orthorectification of the image was performed in order to minimize distortions of the image caused by topography, camera geometry, and other sensor-related errors. RPC file was generated from ephemeris data while the ASTER GDEM data was downloaded from ERSDAC website.

Step 2: Resolution Merge. This step was applied in order to improve the spatial resolution of the multispectral bands of the OrbView-3 image. The PAN band of the GeoEye OrbView-3 with spatial resolution of 1m was merged with the multispectral bands of the same sensor with 4m spatial resolution. Pan-sharpening techniques have been widely used in remote sensing applications in order to improve the quality of the multispectral images (Garzelli and Nencini, 2007). Pan-sharpening is a process of merging high-resolution panchromatic and lower resolution multispectral imagery to create a single high-resolution color image.

Step 3: SAM target detection. The next step was the application of the Spectral Angle Mapper (SAM) for OMW target detection. SAM algorithm was found to be the most promising compared to other known algorithms (not shown in this paper) such as Matched Filtering; Constrained Energy Minimization; Adaptive Coherence Estimator etc. A small sample (Region Of Interest-ROI) was selected from a known OMW disposal site while other not-OMW ROIs have been also selected to improve the quality of the results.

Step 4: Filtering (Sieving & Clumping). Although SAMs' high performance a significant amount of pixels within the image -candidate as potential OMW areas- will remain. For this reason a threshold and filtering of the image was necessary. Sieving filtering was applied to solve the problem of isolated pixels occurring in classification images (i.e. less than 2 pixels) while with clumping filtering similar classified areas were adjusted together using morphological operators.

Step 5: Masking using topographical parameters. Using the ASTER GDEM dataset the slope of the case study area was calculated in a GIS environment. Then areas with slope more than 20% (hilly areas) were excluded (masked) from the analysis since OMW disposal areas are located in flat or almost flat regions.

Step 6: Querying image using geometric properties. Area and length properties of the remaining candidate pixels have been calculated in the GIS environment. Then SQL query has been applied based on specific geometric and shape properties in order to further exclude the remaining areas.

Step 7: Accuracy assessment. The final step for this semi-automatic approach was the accuracy assessment of the results. For this reason the detected OMW disposal areas have been compared with known OMW areas of the region.

b. Case study area 2: *Mironikitas* area

In the second area GE images have been exploited. GE releases free images in high spatial resolution that may provide some potential for regional land use/cover mapping as well for the detection of objects in inaccessible sites. GE provides very high resolution (VHR) natural-colour (red-green-blue, RGB) images based on commercial space borne sensors. Although the several limitations than GE images have (e.g.

compression of the original satellite images; loss of image quality; no NIR band is provided etc.) it is worth to note that several researchers have already identify the great potential of GE (and similar digital globes) to support research and to provide updated information (Ghaffarian and Ghaffarian, 2014; Kennedy and Bishop, 2011).

While interpretation of these freely distributed high resolution images can be accurate enough this procedure is time-consuming. Hence automatic procedures can be alternative used. A variety of well-known classification algorithms such as Minimum Distance (MD); Maximum Likelihood (ML); Mahalanobis Distance; Spectral Angle Mapper (SAM) as well Support Vector Machine (SVM) have been evaluated for the *Mironikitas* area. Moreover different scales of GE images have been evaluated in order to examine the impact of scale to the classification accuracy (i.e. detection of OMW disposal areas).

4. RESULTS

a. Case study area 1: *Mesaras* inlet

Initially the high resolution GeoEye OrbView-3 satellite (overpass 18 June 2006) was orthorectified using the RCP file and the ASTER GDEM data available for this area. The orthorectification was applied so as to minimize the distortion of the image mainly due to the mountainous topography of region. Then the Brovey transformation was applied so that to improve the spatial resolution of the multispectral image. Brovey pan sharpening technique is one of the simpler but widely-used RGB colour fusion (Zhang, 2004) due to its high degree of spatial enhancement, speed, and ease of implementation (Johnson et al., 2014). The basic procedure of the Brovey transform first multiplies each multispectral band by the high-resolution panchromatic band, and then divides each product by the sum of the multispespectral bands (Nikolakopoulos, 2008).

Furthermore, the SAM target detection algorithm was used. This method treats the spectra as vectors and calculates the spectral angle between the known (OMW area) and the rest of the image. SAM method is insensitive to illumination since the algorithm uses only the vector direction and not the vector length. The result of the SAM classification is an image showing the best match at each pixel.

For this purpose a known OMW disposal area was selected (ROI). To reject background data other ROIs have been also selected. In this way the algorithm was able to distinguish pixels between the target (OMW areas) and background regions. Target finding approach is an iterative approach since the SAM analysis may still produce false positives (data included in a resulting class that do not accurately represent a target). Such misclassification results are mainly observed over water bodies and shadows.

Therefore special focused was given to select representative ROI for OMW disposal areas as well other similar targets that may produce false positive. Another critical parameter was the SAM Maximum Angle field, were the angle defines which pixel may (or may not) classified as OMW areas. Through this process it was found that due to its unique spectral signature of OMW disposal areas (low reflectance values in the visible part of the spectrum ($\rho<5\%$) and relative high reflectance values in the NIR part of the spectrum, ($\rho=10\%$) a minimum SAM angle can be determined. As shown in Figure 2, after the application of SAM detection algorithm a small number of candidate pixels still remains ($\approx 0.03\%$ of the initial dataset). As it is indicated in Figure 2, different coastal areas were found to give false positives while other false true areas can be found mainly in shadowed areas. To further minimize the results a topographic restriction was applied in a GIS environment. The slope of the region was calculated based on the

ASTER GDEM data. Since OMW waste disposal areas are found in mainly flat or almost flat regions a threshold of slope = 20% was used (Figure 2, middle) to mask the results from the SAM detection algorithm (Figure 2).

Figure 2: (a) The semi-automatic identification of OMW disposal areas in the area of *Mesaras* inlet for the different steps of the applied methodology: Initially the orthorectification of the image was performed, and then (b) the SAM detection algorithm was applied. Yellow pixels indicate the candidate areas as OMW disposal areas. Then (c-d) the results were masked based on topographic parameters (slope >20%) while the final stage (e) involved the extraction of OMW sites based on geometric properties. The final three areas as detected from the methodology applied in the *Mesaras* area are shown in the last column (f)

More than 50% of the initial areas have been eliminated from the above step. The final step was to apply geometrical queries to the remaining target areas. Simple geometrical and shape features have been used so that to exclude either very small or very large regions (based on the area), or to ignore targets based on the length of the feature. Moreover shape properties (e.g. area to length parameter) have been also applied so that to exclude no rectangular-like shape areas. The above parameters were applied as SQL query in the remaining dataset in the GIS environment. The final results (Figure 2, right) show that the remaining areas are limited to a small number of 3 potential OMW disposal areas. A closer look to these final results (Figure 2) was able to highlight the proposed methodology. As it is shown in Figure 2 other OMW disposal areas have been spotted automatically from the entire GeoEye OrbView-3 image.

b. Case study area 2: *Mironikitas* area

For the second case study area in the region of *Mironikita* GE high resolution images have been used. The purpose for this case study was to evaluate the potential use of detection of OMW areas using the RGB images from GE engine. Several classification techniques have been evaluated for the purpose of this study. In the literature different supervised or unsupervised classification techniques exist, e.g. per-pixel based maximum likelihood, nearest neighbour, fuzzy classifications, object-oriented multi-resolution segmentation, artificial neural networks, decision tree-based classification, and rule-based classification (Blaschke, 2010; Lillesand, Kiefer and Chipman, 2004; Campbell, 2007; Moutrakis and Ogole, 2011). Using areas of interest, the overall performance of each technique can be measured and evaluated based on statistical analysis.

The MD algorithm is a statistical technique that classifies the image based on the closest distance of training areas using the spectral characteristics of the pixels (Lillesand, Kiefer and Chipman, 2004). Usually it is possible to specify a maximum distance threshold: If the distance is still further away than that threshold, it is assumed that none of the groups is similar enough and the result will be “unknown”. ML algorithm performs classification based on the normal probability density function (Campbell, 2007). The SAM algorithm is an automated method which calculates and classifies the spectral angle between the pixels of the image (Campbell, 2007). SVM is a machine-learning technique that is well adapted to solving non-linear, high dimensional space classifications. As Heumann (2011) argues, SVM can be used for remote sensing applications, for classification of either multispectral or hyperspectral data, in which there is a spectral similarity between the pixels. SVM aims to identify the boundaries between classes in n-dimensional spectral-space (Yuhendra, Sumantyo and Kuze,

2012). As Paneque-Gálvez *et al.* (2013) argue, SVM classifiers have been shown to attain high accuracies in land use cover mapping and outperform other algorithms.
Four different scales have been selected in this area as shown in Figure 3. Figure 3a was captured from a height of approximately 100 meters above the OMW area while Figure 3b was captured from a height of 250 meters over the OMW area. Figure 3c was taken from GE from a height of 850 meters while Figure 3d from a height of approximately 2000 meter over the same area. Red colour indicates the OMW areas; brown and blue colour for the soil areas while green areas for vegetated regions. The classifications results (i.e. Kappa coefficient; Overall accuracy; Producer Accuracy and User Accuracy) for each case are shown in Table 1.

Figure 3: Classification results for the *Mironikita* area in four different scales (I-IV: 100; 250; 850 and 2000 meters above the OMW area respectively). Row (a) corresponds to GE image; (b) for MD classification; (c) ML classification; (d) Mahalanobis classification; (e) SAM classification and (f) SVM classification results. Red colour indicates the OMW areas; brown and blue colour for the soil areas while green areas for vegetated regions.

Scale	Classifier (Kappa Coefficient)				
	MD	ML	Mahal.	SAM	SVM
100	0,33	0,66	0,81	0,53	0,92
250	0,41	0,91	0,92	0,65	0,86
850	0,70	0,96	0,95	0,65	0,91
2000	0,69	0,74	0,77	0,69	0,82

Scale	Classifier (Overall Accuracy)				
	MD	ML	Mahal.	SAM	SVM
100	0,55	0,77	0,86	0,66	0,93
250	0,52	0,92	0,92	0,76	0,92
850	0,76	0,92	0,93	0,73	0,92
2000	0,73	0,74	0,84	0,82	0,89

Scale	Classifier (Producer Accuracy)				
	MD	ML	Mahal.	SAM	SVM
100	26,25	60,92	83,44	53,92	93,44
250	42,07	78,91	92,47	69,66	82,93
850	61,44	96,21	95,69	62,40	87,11
2000	48,21	88,56	72,17	54,37	85,00

Scale	Classifier (User Accuracy)				
	MD	ML	Mahal.	SAM	SVM
100	61,25	86,97	90,94	74,91	93,12
250	40,84	89,60	91,91	79,25	91,33
850	87,01	92,36	92,83	89,54	94,36
2000	79,41	75,28	87,26	80,65	87,81

Table 1: Kappa coefficient; Overall accuracy; Producer accuracy and User accuracy are provided for the classification results using different classifiers at the *Mironikita* area in four different scales: 100m; 250m; 850m and 2000m

Accuracy assessment has been a topic of considerable debate and research in remote sensing for many years. This is in part because the promoted standard methods such as the kappa coefficient are not always appropriate (Foody, 2002). Several researchers have worked on these problems of accuracy assessment and analysis of the classification uncertainty (Olofsson *et al.,* 2013; 2014; Liu *et al.,* 2007). In this paper some established accuracy measures for OMW areas are also provided. As shown in Figures 3 and Table 1, classification accuracy is not directly related with the scale of the image. Indeed as seen for instance in Figure 3a (MD classifier) OMW area was more accurate classified in the lower scale (Figure 3b-3c, MD classifier). This is case for the rest of the classifiers as well. As several studies have presented the optimal spatial resolution is not essentially associated with the highest spatial resolution satellite imagery. This is generally the case in heterogeneous areas (such as OMW areas) where the optimal pixel size is influenced by the spatial structure of the investigated objects

and the image processing designs, e.g., spectral classification, regression, texture analysis etc. (Tran *et al.,* 2011). As Woodcock and Strahler (1987) suggest an appropriate scale for observation is a function of the type of environment and the kind of information desired. The choice of scale is therefore determined by the size of the studied area and the type of phenomena analysed.

SVM classifier has shown the best overall performance and stability for detection of the OMW areas regardless the scale of the image taken from Google Earth. In contrast MD classifier tend to give poor results for all scales (kappa coefficient < 0.70) while SAM classification provides better results as the image was captured from a higher point (see Table 1). In contrary ML classification tends to give poor results for very near as well very distance height (Figures 3a - 3d). The results show that the optimum height for the majority of the classifications is from heights of 850 meters (see Table 1) suggesting that this height can be used for other areas as well to classify (and therefore detect) OMW areas from Google Earth images.

5. CONCLUSIONS

Olive oil industry is very important in Mediterranean countries. Greece is the 3rd major olive oil producers worldwide. However the extraction of olive oil generates huge quantities of wastes which can be harmful for the environment. More than 5% of the oil worldwide production is produced in the island of Crete. In this region almost 1000 OMW disposal areas have been recorded. These OMW disposal areas are scattered all over the island while their identification might be difficult and time consuming if this is based only from in –situ observations.

For this reason alternative ways to detect as well to monitor OMW areas should be studied. In this direction, remote sensing techniques may be used as an essential and economic tool for detection of OMW disposal areas. In this paper freely distributed high resolution satellite images have been explored in two different cases studies. In the first case study area a GeoEye OrbView-3 image was used in order to semi-automatic detect potential OMW areas. The detection was based on the SAM detection classifier while both topographical and geometrical attributes where used to support this methodology. The results were found very promising since 4 OMW areas where detected in this region with coverage of approximately 240 square kilometres.

In the second case study the Google Earth engine was used to examine if such RGB freely distributed images can be used to detect disposal areas. Several classification algorithms have been applied in different scales. The results indicated that complicated classifiers such as SVM can be sufficiently used to extract OMW areas from a height of 850 meters from the GE digital globe. Although training areas (ROIs) are needed for both methodologies, the unique spectral profile of OMW areas can be sufficiently used in conjunction with GIS spatial analysis and SQL queries to identify OMW area.

ACKNOWLEDGMENTS

This work was performed in the framework of the PEFYKA project within the KRIPIS Action of the GSRT. The project is funded by Greece and the European Regional Development Fund of the European Union under the NSRF and the O.P. Competitiveness and Entrepreneurship.

REFERENCES

ALEXAKIS, D.D., SARRIS, A., KALAITZIDIS, C., PAPADOPOULOS, N. AND SOUPIOS, P., 2015. Integrated use of satellite remote sensing, GIS and ground spectroscopy techniques for monitoring olive oil mill waste disposal areas in Crete Island –Greece. *International Journal of Applied Earth Observation and Geoinformation,* (submitted).

ASFI, M., OUZOUNIDOU, G., PANAJIOTIDIS, S., THERIOS, I. AND MOUSTAKAS, M., 2012. Toxicity effects of olive-mill wastewater on growth, photosynthesis and pollen morphology of spinach plants. *Ecotoxicology and Environmental Safety,* 80(1), 69-75,

BLASCHKE, T., 2010. Object based image analysis for remote sensing. *ISPRS Journal of Photogrammetry and Remote Sensing*, 65(1),2-16.

CAMPBELL, J. B., 2007. *Introduction to Remote Sensing*, The Guilford Press, New York, 2007

CAMARSA, G., GARDNER, S., JONES, W., ELDRIDGE, J., HUDSON, T., THORPE, E. AND O"HARA, E., 2010. Good practice in improving environmental performance in the olive oil sector. *Luxembourg: Office for Official Publications of the European Union.*

DELLAGRECA, M., MONACO, P., PINTO, G., POLLIO, A., PREVITERA, L. AND TEMUSSI, F., 2001. Phytotoxicity of low-molecular-weight phenols from olive mill wastewaters. *Bulletin of Environmental Contamination and Toxicology*, 67, 352–359.

FOODY, M. G., 2002. Status of land cover classification accuracy assessment. *Remote Sensing of Environment,* 80,185– 201

GARZELLI, A. AND NENCINI, F., 2007. Panchromatic sharpening of remote sensing images using a multiscale Kalman filter. *Pattern Recognition* **40(12)**, pp. 3568-3577

GHAFFARIAN, S. AND GHAFFARIAN, S., 2014. Automatic building detection based on Purposive FastICA (PFICA) algorithm using monocular high resolution Google Earth images. *ISPRS Journal of Photogrammetry and Remote Sensing*, 97, 152-159.

HEUMANN, B.W., 2011. An object-based classification of mangroves using a hybrid decision tree-Support Vector Machine approach. *Remote Sensing,* 3, 2440-2460.

JOHNSON, A. B., SCHEYVENS, H. AND SHIVAKOTI, R. B., 2014. An ensemble pansharpening approach for finer-scale mapping of sugarcane with Landsat 8 imagery. International Journal of Applied Earth Observation and Geoinformation, 33, 218-225

KENNEDY, D. AND BISHOP, M.C., 2011. Google earth and the archaeology of Saudi Arabia. A case study from the Jeddah area. *Journal of Archaeological Science*, 38(6), 1284-1293

MOUNTRAKIS, G., IM, J. AND OGOLE, C., 2011. Support vector machines in remote sensing: A review. *ISPRS Journal of Photogrammetry and Remote Sensing*, 66 (3) 247-259.

LILLESAND, T. M., KIEFER, R. W. AND CHIPMAN, J., 2004. *Remote Sensing and Image Interpretation*, Lehigh Press, 2004.

LIU, C., FRAZIER, P. AND KUMAR. L., 2007. Comparative assessment of the measures of thematic classification accuracy. *Remote Sensing of Environment,* 107, 606–616

NIAOUNAKIS, M. AND HALVADAKIS, C. P., 2006. Olive processing waste management. Literature review and patent survey. *Waste Management Series*, 5, Elsevier Ltd.

NIKOLAKOPOULOS, G. K., 2008. Comparison of nine fusion techniques for very

high resolution data. *Photogrammetric Engineering & Remote Sensing*, **74(5)**, pp. 647–659.

NTOUGIAS, S., GAITIS, F., KATSARIS, P., SKOULIKA, S., ILIOPOULOS, N. AND ZERVAKIS, I.Z., 2013. The effects of olives harvest period and production year on olive mill wastewater properties – Evaluation of Pleurotus strains as bioindicators of the effluent's toxicity. *Chemosphere*, 92(4), 399-405.

OLOFSSON, P., FOODY, M. D., STEHMAN, V. S., AND WOODCOCK E. C., 2013. Making better use of accuracy data in land change studies: Estimating accuracy and area and quantifying uncertainty using stratified estimation. *Remote Sensing of Environment,* 129, 122–131.

OLOFSSON, P., FOODY, M. D., STEHMAN, V. S., WOODCOCK E. C. AND WULDER, M. A., 2014. Good practices for estimating area and assessing accuracy of land change. *Remote Sensing of Environment,* 148, 42–57.

PANEQUE-GÁLVEZ, J., MAS, J.-F., MORÉ, G., CRISTÓBAL, J., ORTA-MARTÍNEZ, M., LUZ, C.A., GUÈZE, M., MACÍA, J. M. AND REYES-GARCÍA, V., 2013. Enhanced land use/cover classification of heterogeneous tropical landscapes using support vector machines and textural homogeneity. *International Journal of Applied Earth Observation and Geoinformation*, 23, 372-383.

PAREDES, M.J., MORENO, E., RAMOS-CORMENZANA, A. AND MARTINEZ, J.. 1987. Characteristics of soil after pollution with wastewaters from olive oil extraction plants. *Chemosphere*, 16 (7), 1557–1564.

ROIG, A., CAYUELA, M.L. AND SÁNCHEZ-MONEDERO, M.A., 2006. An overview on olive mill wastes and their valorisation methods. *Waste Management*, 26(9), 960-969.

TRAN, T.-B., PUISSANT, A., BADARIOTTI, D. AND WEBER, C., 2011. Optimizing Spatial Resolution of Imagery for Urban Form Detection—The Cases of France and Vietnam. *Remote Sensing,* 3(10), 2128-2147.

USGS, 2014. OrbView-3. https://lta.cr.usgs.gov/satellite_orbview3

WOODCOCK, C.E. AND STRAHLER, A.H., 1987. The factor scale in remote sensing. *Remote Sensing of Environment,* 21, 311-332.

YUHENDRA, A. I., SUMANTYO, S.T.J. AND KUZE, H., 2012. Assessment of pan-sharpening methods applied to image fusion of remotely sensed multi-band data. *International Journal of Applied Earth Observation and Geoinformation*,18165-175, 10.1016/j.jag.2012.01.013.

ZHANG, Y., 2004. Understanding image fusion. *Photogrammetric Engineering & Remote Sensing*, **70(6)**, pp. 657–661.

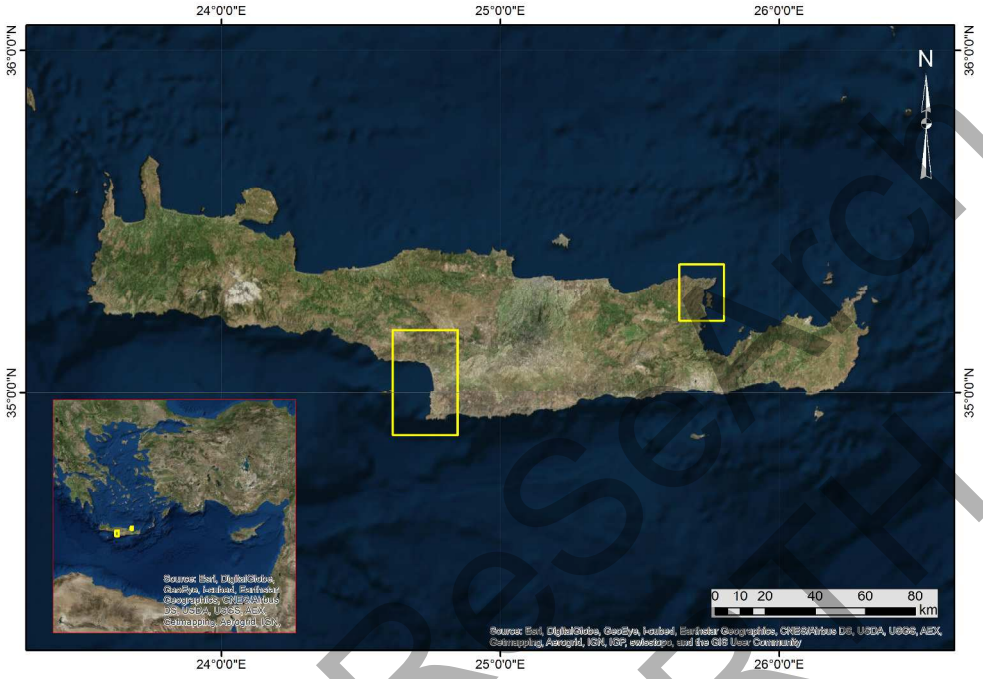

Figure 1. The two cases studies area in the island of Crete. The 1st case study (indicated with yellow square in the central-southern part of Crete) a high resolution GeoEye OrbView-3 satellite image was used while for the 2nd case study (indicated with yellow square in the eastern-northern part of Crete) GE images have been explored.
297x210mm (300 x 300 DPI)

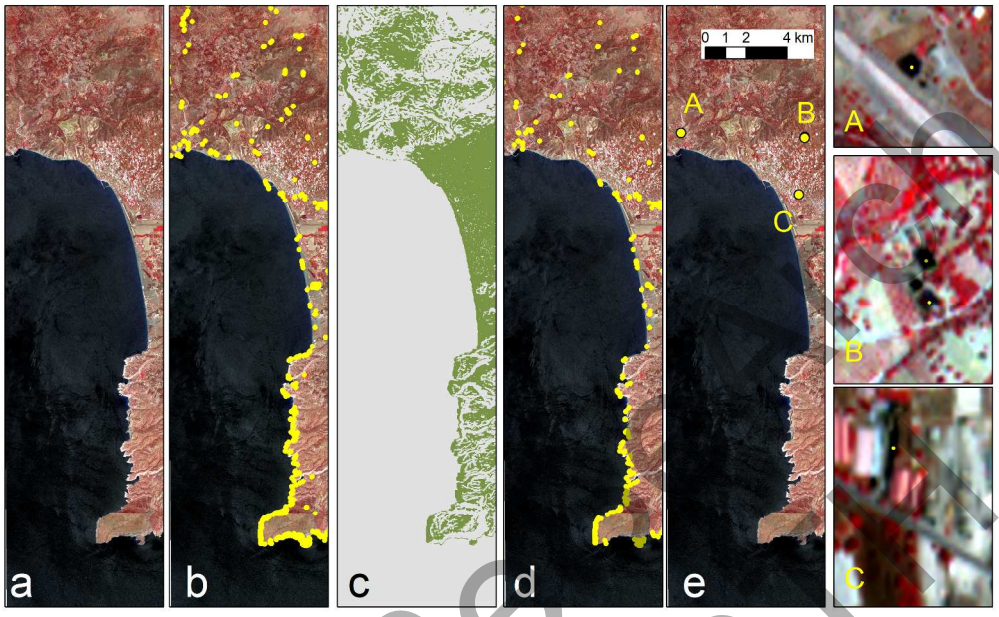

(a) The semi-automatic identification of OMW disposal areas in the area of Mesaras inlet for the different steps of the applied methodology: Initially the orthorectification of the image was performed, and then (b) the SAM detection algorithm was applied. Yellow pixels indicate the candidate areas as OMW disposal areas. Then (c-d) the results were masked based on topographic parameters (slope >20%) while the final stage (e) involved the extraction of OMW sites based on geometric properties. The final three areas as detected from the methodology applied in the Mesaras area are shown in the last column (f)
292x182mm (300 x 300 DPI)

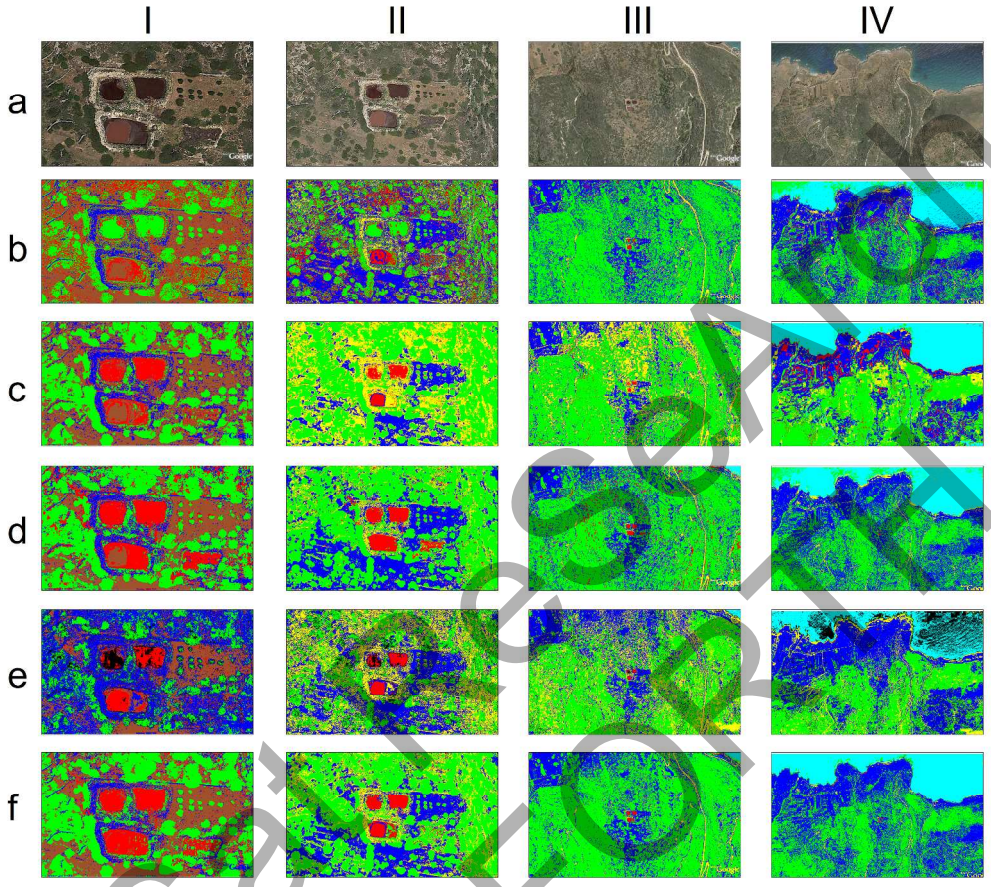

Classification results for the Mironikita area in four different scales (I-IV: 100; 250; 850 and 2000 meters above the OMW area respectively). Row (a) corresponds to GE image; (b) for MD classification; (c) ML classification; (d) Mahalanobis classification; (e) SAM classification and (f) SVM classification results. Red colour indicates the OMW areas; brown and blue colour for the soil areas while green areas for vegetated regions.
457x410mm (300 x 300 DPI)